Supramolecular Capsules

Deutsche Ausgabe: DOI: 10.1002/ange.201607789
Internationale Ausgabe: DOI: 10.1002/anie.201607789

[N···I$^+$···N] Halogen-Bonded Dimeric Capsules from Tetrakis(3-pyridyl)ethylene Cavitands

*Lotta Turunen, Ulrike Warzok, Rakesh Puttreddy, Ngong Kodiah Beyeh, Christoph A. Schalley, and Kari Rissanen**

Abstract: *Two [N···I$^+$···N] halogen-bonded dimeric capsules using tetrakis(3-pyridyl)ethylene cavitands with different lower rim alkyl chains are synthesized and analyzed in solution and the gas phase. These first examples of symmetrical dimeric capsules making use of the iodonium ion (I$^+$) as the main connecting module are characterized by ^{1}H NMR spectroscopy, diffusion ordered NMR spectroscopy (DOSY), electrospray ionization mass spectrometry (ESI-MS), and ion mobility-mass spectrometry (TW-IMS) experiments. The synthesis and effective halogen-bonded dimerization proceeds through analogous dimeric capsules with [N···Ag$^+$···N] binding motifs as the intermediates as evidenced by the X-ray structures of* $(CH_2Cl_2)_2$@[**3a**$_2$·Ag_4·$(H_2O)_2$·OTs_4] *and* $(CH_2Cl_2)_2$@[**3a**$_2$·Ag_4·$(H_2O)_4$·OTs_4]*, two structurally different capsules.*

Resorcinarene cavitands are pre-organized macrocyclic compounds with concave cavities large enough to accommodate small organic molecules or ions.[1–3] Cavitands are widely used receptors in supramolecular chemistry since the size, shape, rigidity, and electronic properties of the cavity can be modified by using different bridging groups and by adjusting functional groups at different positions on the cavitand, for example, at the 2-position of the phenyl ring or the lower rim.[1,2,4–6] In addition to their receptor properties, cavitands are suitable supramolecular synthons for the construction of capsular and larger supramolecular assemblies.[1,2,4–7] Since the seminal work of Cram,[1] a multitude of self-assembled capsules through different non-covalent interactions has been reported.[4–6,8–13] Dimeric capsules through hydrogen bonding, ionic interactions, metal–ligand coordination, and recently through halogen bonding have been constructed, utilizing tetrafunctionalized cavitands.[4–6,8–14]

Halogen bonding (XB) results from the non-covalent interaction between polarized halogen atoms and Lewis bases.[15] They can be used to form highly directional interactions in the solid state, in solution as well as in the gas phase, which makes them useful tools in the design of supramolecular architectures.[16] Halonium ions are not only interesting synthetic intermediates, but also useful XB donors, which are able to make three-center-four-electron bonds,[17–20] also known as halogen bonds with coordinative nature,[21] with two acceptor moieties. Their use in XB complexes was first reported by Erdelyi and co-workers.[17,19] In these [N···X$^+$···N] complexes, the halonium ion is simultaneously stabilized by two electron-donating pyridine groups or pyridine derivatives. The [N···I$^+$···N] XBs of [bis(pyridine)iodonium]$^+$ and [1,2-bis(pyridine-2-ylethynyl)benzeneiodonium]$^+$ complexes are shown to be symmetric, independent of the nature of the counterion present and exceptionally strongly bound in solution as well as in the solid state.[17–20]

Although many halogen-bonded supramolecular architectures have been reported in the last decades,[16] halogen-bonded capsular assemblies are rare. Recent examples are the dimeric pseudo-capsular XB complex between a rigid tetrakis(3-pyridyl)cavitand and a flexible tetrakis(4-iodotetrafluorophenyl)calix[4]arene,[22] and a dimeric capsule based on cavitands with 2,3,5,6-tetrafluoro-4-halophenyl and pyridyl moieties.[14] We have recently reported the use of *N*-alkyl ammonium resorcinarene salts as XB acceptors to construct a dimeric capsule with molecular iodine as the XB donor.[23]

Halonium-based XB systems have not been applied so far in the construction of larger supramolecular assemblies. The coordinative nature[21] of the halonium ion, coupled with their ability to form directional and divalent XB complexes makes them suitable building blocks for cavity containing assemblies. We envisaged that the combination of two directional cavitands as tetratopic XB acceptors and the iodonium ions (I$^+$) as the divalent linear XB donor should result in capsular architectures. Herein, we present the first examples of dimeric capsules formed from two tetrakis(3-pyridyl)ethylene cavitands and iodonium ions, supplemented with the corresponding intermediate isoelectronic Ag$^+$-capsules. In contrast to the more rigid methylene-bridged cavitands, the studied ethylene cavitands offer the correct spatial arrangement of the XB acceptor moieties, which, in combination with the linear [N···X$^+$···N] geometry, will lead to the dimeric XB capsules. Cavitands with two different lower rim alkyl chains were used owing to the difference in solubility and crystallization behavior.

The tetratopic XB acceptors **3a** and **3b** (Scheme 1) were synthesized by Suzuki-coupling of 3-pyridylboronic acid to tetrahalogenated ethylene cavitands (see Supporting information for details of the synthesis).[24] The positive mode

---

[*] M. Sc. L. Turunen, Dr. R. Puttreddy, Acad. Prof. K. Rissanen
Department of Chemistry, NanoScience Center
University of Jyvaskyla
P.O. Box 35, FI-40014 Jyvaskyla (Finland)
E-mail: kari.t.rissanen@jyu.fi

M. Sc. U. Warzok, Prof. C. A. Schalley
Institut für Chemie und Biochemie der Freien Universität Berlin
Takustrasse 3, 14195 Berlin (Germany)

Dr. N. K. Beyeh
Aalto University, School of Science, Department of Applied Physics
Puumiehenkuja 2, FI-02150, Espoo (Finland)

Supporting information and the ORCID identification number(s) for the author(s) of this article can be found under http://dx.doi.org/10.1002/anie.201607789.

© 2016 Wiley-VCH Verlag GmbH & Co. KGaA, Weinheim

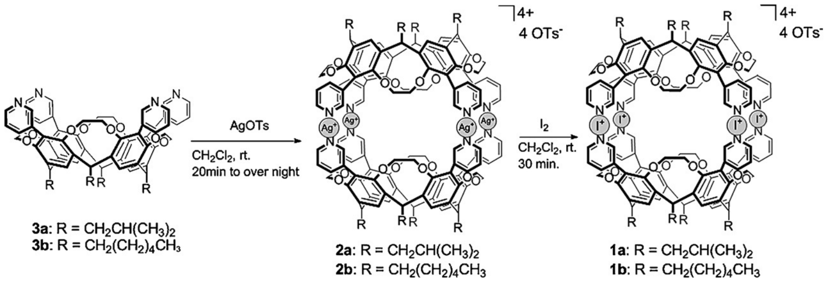

Scheme 1. Syntheses of the Ag$^+$ (**2a** and **2b**) and I$^+$ (**1a** and **1b**) capsules.

electrospray ionization (ESI$^+$) mass spectra of **3a** and **3b** show the singly and doubly protonated monomers as well as some sodium adducts. No dimers or higher aggregates from **3a** or **3b** were observed when sprayed from protic solvents (Figure S7 in the Supporting Information).

The reaction between cavitands **3a** and **3b** with silver(I) *p*-toluenesulfonate (AgOTs) in 1:2 ratio in dichloromethane gave the dimeric silver capsules **2a** and **2b** (Scheme 1). The Ag$^+$-bridged dimeric capsule **2a** shows a complex ^{1}H NMR spectrum (Figure 1b, for **2b** see Figure S5), suggesting a mixture of self-assembled Ag$^+$-complexes, most likely dimeric in nature. This is also supported by the X-ray structure of **2a**, which manifests two structurally different capsules (see X-ray discussion and Figure 2), and the ^{1}H diffusion ordered NMR (DOSY) measurements, which show at least two discrete dimeric species for both capsules **2a** and **2b** (Figure S5). The ESI-MS spectra of Ag$^+$-capsules **2a** and **2b** reveal intact dimeric complexes as the $[\mathbf{3a}_2\cdot\mathrm{Ag}_4\cdot\mathrm{OTs}_2]^{2+}$ and $[\mathbf{3b}_2\cdot\mathrm{Ag}_4\cdot\mathrm{OTs}_2]^{2+}$ ions at *m/z* 1512 and 1624, respectively (Figure S8). The collision-induced dissociation (CID) tandem MS experiments performed on mass-selected ions show predominantly the symmetric fragmentation of the capsules into their monomers $[\mathbf{3a}\cdot\mathrm{Ag}_2\cdot\mathrm{OTs}]^+$ and $[\mathbf{3b}\cdot\mathrm{Ag}_2\cdot\mathrm{OTs}]^+$ which further eliminate AgOTs to yield $[\mathbf{3a}\cdot\mathrm{Ag}]^+$ and $[\mathbf{3b}\cdot\mathrm{Ag}]^+$, respectively (Figure S10).

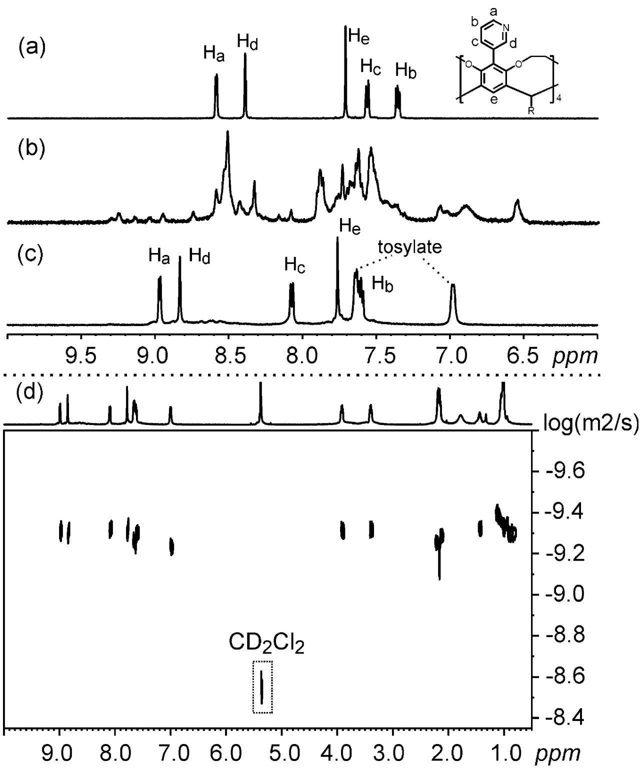

Figure 1. Selected region of the ^{1}H NMR spectra (CD$_2$Cl$_2$, 500 MHz, 298 K) of a) **3a**, b) **2a** and c) **1a**, and d) the ^{1}H DOSY NMR spectrum of **1a**.

Addition of molecular iodine to **2a** and **2b** in dichloromethane solution led to the precipitation of AgI and in situ generation of I$^+$ which reacted with the cavitands to give [N···I$^+$···N]-bridged dimeric capsules **1a** and **1b**. Their ^{1}H NMR spectra show only one set of well-resolved signals for all pyridine protons, which are shifted downfield compared to the signals of the respective free cavitand (Figure 1). This result indicates a symmetrical assembly with [N···I$^+$···N] halogen bonds (Figure 1c). To obtain more evidence of the formation of the iodonium-bridged capsules, diffusion ordered NMR (DOSY) experiments were performed. The ^{1}H DOSY measurements in dichloromethane at 298 K for cavitands **3a** and **3b** gave diffusion coefficients of $7.5\times10^{-10}\,\mathrm{m^2\,s^{-1}}$ and $6.9\times10^{-10}\,\mathrm{m^2\,s^{-1}}$, respectively. For the iodonium capsules, the ^{1}H DOSY analyses reveal one set of signals with considerably lower diffusion coefficient of $4.8\times10^{-10}\,\mathrm{m^2\,s^{-1}}$ for **1a** (Figure 1d) and $4.6\times10^{-10}\,\mathrm{m^2\,s^{-1}}$ for **1b** (Figure S6) indicating the formation of larger assemblies. Assuming the complexes formed are roughly spherical, the hydrodynamic radius *r* can be calculated from the Stokes–Einstein equation (Table S1) resulting in the diameter sizes of 1.42, 1.54, 2.22, and 2.32 nm for **3a**, **3b**, **1a**, and **1b**, respectively.

Single crystals of the dimeric capsule **2a** were obtained by slow evaporation from a wet dichloromethane/acetonitrile solution. The crystal lattice contains two structurally different centrosymmetric dimeric capsules **2a_A** and **2a_B** (Figure 2) and thus it could be considered as a co-crystal with two structurally different capsules. The difference between **2a_A** and **2a_B** comes from the different Ag-coordination and the amount of coordinated water molecules. The capsule **2a_A** has two different Ag-centers, a 4-coordinate pseudo-tetrahe-

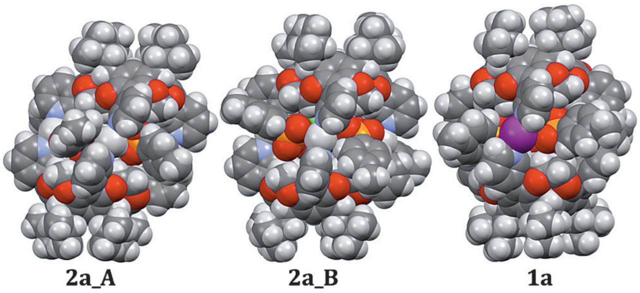

Figure 2. The crystal structures of the capsules **2a_A** and **2a_B**, and the modelled structure of the iodonium capsule **1a**. dark gray C, small light gray H, large light gray Ag, purple I, blue N, red O, orange S, green Cl.

© 2016 Wiley-VCH Verlag GmbH & Co. KGaA, Weinheim

dral N_2O_2 [two pyridines and two tosylates] and a 3-coordinate planar N_2O [two pyridines and one water molecule], while the capsule **2a_B** is more symmetric with each Ag^+ having pseudo-tetrahedral N_2O_2 coordination from two pyridine groups, one tosylate, and one water molecule (Figure S14). Thus the **2a_A** is formally a dihydrate $(CH_2Cl_2)_2@[\mathbf{3a}_2\cdot Ag_4\cdot(H_2O)_2\cdot OTs_4]$ and the **2a_B** a tetrahydrate $(CH_2Cl_2)_2@[\mathbf{3a}_2\cdot Ag_4\cdot(H_2O)_4\cdot OTs_4]$. Both capsules tightly entrap two dichloromethane molecules, but owing to the different coordination around the Ag^+-centers, the cavity structures are slightly different. This results in different cavity volumes of the capsules (Figures S15 and S16) of 207 and 223 Å^3 using a 1.75 Å probe[25–27] for **2a_A** and **2a_B**, respectively (Table S2), leading to packing coefficients 0.59 (**2a_A**) and 0.52 (**2a_B**).

Possibly due to the different coordination behavior of the I^+ cation, we have not been able to crystallize and obtain an X-ray structure of the target tetra-iodonium capsule, **1a**. Using the known coordination geometry of the $[N\cdots I^+\cdots N]$ moiety[17–20] {N–I$^+$ bond of 2.25 Å and $N\cdots I^+\cdots N$ angle of 180°} a molecular model of **1a** was optimized on a MM level using SPARTAN2014 program[28] (Figure 2, Figure S17). The optimized structure of **1a** is very close to that of the more symmetric capsule **2a_B** (Figure 2). The size of all the capsules, **1a**, **2a_A**, and **2a_B**, is very similar: 2.1 × 2.1 × 2.5 nm. This value is in perfect agreement with the DOSY NMR values obtained for **1a** (Figure 1 d).

Electrospray ionization mass spectrometry (ESI-MS) measurements provide clear evidence of the selective formation of the halogen-bonded capsules **1a** and **1b**. For capsule **1a**, signals of different charge-states with two cavitands **3a** and four, three, or two iodonium ions are observed (Figure 3 a). The base peak of the spectrum at m/z 1549 can be assigned to the species $[\mathbf{3a}_2\cdot I_4\cdot OTs_2]^{2+}$. The observed exact mass and experimental isotope pattern agree with those simulated based on natural abundances (Figure 3 b). The presence of the singly protonated complex $[\mathbf{3a}_2\cdot I_3\cdot H\cdot OTs_2]^{2+}$ at m/z 1486 is probably due to the presence of an open coordination site in the capsule with less than four bound I^+ ions. The ESI-MS results also clearly show the formation of capsule **1b** in the manner as described for **1a** (Figure S9).

For all the observed ions derived from dimeric I^+-bridged capsules **1a** and **1b**, the maximum and furthermore optimal number of bound I^+ ions is four, strongly indicating a closed capsular structure with four well-defined binding motifs. Moreover, the stability of capsules **1a** and **1b** in solution is high since samples of both compounds gave identical ESI-MS spectra after several days. Collision-induced dissociation (CID) experiments were performed on mass-selected $[\mathbf{3b}_2\cdot I_4\cdot(OTs)_2]^{2+}$ ions derived from capsule **1b** as a representative example to investigate its gas-phase stability. The predominant fragmentation pathway is a stepwise elimination of two neutral I·OTs ion pairs, giving rise to the doubly charged $[\mathbf{3b}_2\cdot I_2]^{2+}$ iodonium-bridged dimer (Figure S10c). This strongly contrasts the corresponding CID experiments on Ag^+-bridged capsules **2a** and **2b**, which showed a charge-separating fragmentation of the doubly charged capsule. These results demonstrate that the gas-phase stability of the halogen-bonded capsule **1b** is significantly higher than those of the corresponding metal coordinated capsules and that two $[N\cdots I^+\cdots N]$ interactions are sufficient to maintain an intact capsule.

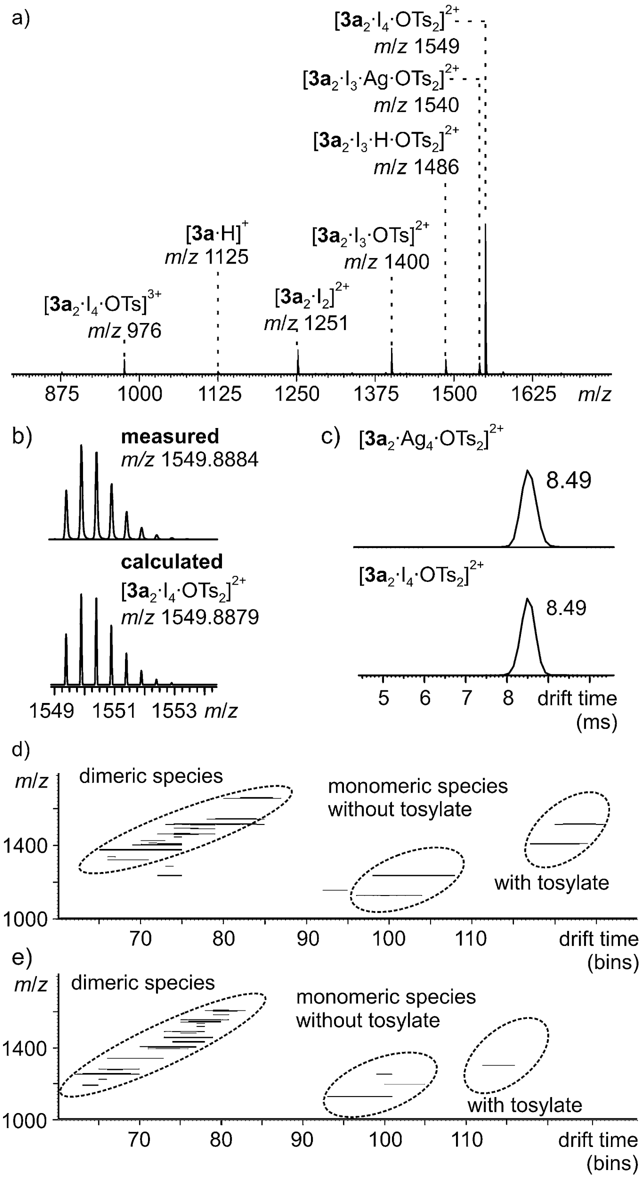

Figure 3. a) ESI-Q-TOF-HRMS spectrum of capsule **1a** (100 μM in CH_2Cl_2), b) experimental and calculated isotopic patterns of the $[\mathbf{3a}_2\cdot I_4\cdot OTs_2]^{2+}$ dication at m/z 1549, c) top: TW-IMS mobilogram of $[\mathbf{3a}_2\cdot Ag_4\cdot OTs_2]^{2+}$ dication derived from capsule **2a**; bottom: TW-IMS mobilogram of $[\mathbf{3a}_2\cdot I_4\cdot OTs_2]^{2+}$ dication derived from capsule **1a**. d) TW-IMS m/z versus drift time plot of capsule **2a**, e) TW-IMS m/z versus drift time plot of capsule **1a**.

To gain more detailed information about the ion structures in the gas phase, travelling-wave ion mobility-mass spectrometry (TW-IMS) was applied. This technique enables the two-dimensional separation of ions depending on their collision cross section as a measure of different sizes and shapes and their mass-to-charge ratio. For Ag^+-bridged capsule **2a**, the examined dimeric complexes exhibit drift times in the range from 7.35 to 8.49 milliseconds (Figure 3 c,

© 2016 Wiley-VCH Verlag GmbH & Co. KGaA, Weinheim

top and Figure S11a). The mobilograms of complexes with four cations are narrow and symmetrical. The *m*/*z* versus drift time plot of capsule **2a** shows three distinct groups of signals, which can be assigned to monomeric cavitand species with and without a *p*-toluenesulfonate anion as well as dimeric capsular species. A linear trend of drift times with increasing mass is apparent for the group of dicationic, dimeric complexes, which differ in the number of bound Ag^+ and *p*-toluenesulfonate anions (Figure 3d). Thus, the same well-defined gas-phase conformation can be assumed for dimeric Ag^+-bridged capsules. The observed ions of I^+-bridged capsule **1a** feature drift times in the range from 6.98 to 8.49 milliseconds (Figure 3c, bottom and Figure S11b). The mobilograms of complexes with four and three I^+ cations display well-defined gas-phase structures whereas those of $[\mathbf{3a}_2\cdot\mathrm{I}_2]^{2+}$ and $[\mathbf{3a}_2\cdot\mathrm{I}_2\cdot\mathrm{H}\cdot\mathrm{OTs}]^{2+}$ indicate the presence of different conformers or regioisomers which differ in the cation arrangement along the rim of the cavitands (Figure S11b). The linear trend of the dimer signals in the *m*/*z* versus drift time plot demonstrates that these species again belong to a group with the same gas-phase conformation (Figure 3e). The absolute drift times of the corresponding **2a** and **1a** capsule ions $[\mathbf{3a}_2\cdot\mathrm{Ag}_4\cdot\mathrm{OTs}_2]^{2+}$ and $[\mathbf{3a}_2\cdot\mathrm{I}_4\cdot\mathrm{OTs}_2]^{2+}$ obtained under identical TW-IMS conditions are equal (8.49 ms). Consequently, we conclude they both have very similar capsular structures, supported by the X-ray structure of **2a_A/B** and molecular modelling of **1a**. The TW-IMS studies on capsules **1b** and **2b** also provide evidence for well-defined and again very similar gas-phase structures for both capsule types with drift times for $[\mathbf{3b}_2\cdot\mathrm{Ag}_4\cdot\mathrm{OTs}_2]^{2+}$ and $[\mathbf{3b}_2\cdot\mathrm{I}_4\cdot\mathrm{OTs}_2]^{2+}$ of 10.14 and 10.47 milliseconds.

In summary, we present the first supramolecular capsules stabilized by four symmetrical $[\mathrm{N}\cdots\mathrm{I}^+\cdots\mathrm{N}]$ halogen bonds. Comprehensive solution and gas-phase studies using ^{1}H NMR, DOSY NMR, ESI-MS, and TW-IMS demonstrate the selective formation of dimeric halogen-bonded capsules **1a** and **1b** upon reaction of the tetrakis(3-pyridyl)ethylene cavitands **3a** and **3b**, first with silver(I) *p*-toluenesulfonate and subsequently with molecular iodine. The DOSY measurements confirm the formation of the I^+-bonded capsules **1a** and **1b** in solution. The gas-phase structure and the $[\mathrm{N}\cdots\mathrm{I}^+\cdots\mathrm{N}]$ binding mode have been confirmed by comparative TW-IMS studies between the halogen-bonded capsules **1a** and **1b** and their corresponding silver-coordinated dimeric precursor capsules **2a** and **2b**. These results clearly show, also in combination with the X-ray crystal structure of the Ag^+-bridged capsules **2a_A** and **2a_B**, that the halogen-bonded capsules are well-defined and stable supramolecular assemblies solely based on robust $[\mathrm{N}\cdots\mathrm{I}^+\cdots\mathrm{N}]$ halogen bonds.

Acknowledgements

We gratefully acknowledge the Academy of Finland (K.R.: grant no. 263256, 265328, 292746, N.K.B.: grant no. 258653, Centre of Excellence HYBER 2014-2019), University of Jyväskylä, Aalto University, the DFG (CRC 1109), and Freie Universität (U.W. and C.A.S.) Berlin for financial support.

Keywords: cavitands · dimeric capsules · halogen bonds · halonium ions · mass spectrometry

How to cite: *Angew. Chem. Int. Ed.* **2016**, *55*, 14033–14036
Angew. Chem. **2016**, *128*, 14239–14242

---

[1] D. J. Cram, *Science* **1983**, *219*, 1177–1183.
[2] J. R. Moran, S. Karbach, D. J. Cram, *J. Am. Chem. Soc.* **1982**, *104*, 5826–5828.
[3] D. J. Cram, J. M. Cram, J. F. Stoddart, *Container Molecules and Their Guests*, The Royal Society Of Chemistry, Cambridge, **1997**.
[4] T. Heinz, D. M. Rudkevich, J. Rebek, Jr., *Nature* **1998**, *394*, 764–766.
[5] D. M. Rudkevich, J. Rebek, Jr., *Eur. J. Org. Chem.* **1999**, 1991–2005.
[6] A. Gissot, J. Rebek, Jr., *J. Am. Chem. Soc.* **2004**, *126*, 7424–7425.
[7] H. Xi, C. L. D. Gibb, *Chem. Commun.* **1998**, 1743–1744.
[8] S. M. Biros, J. Rebek, Jr., *Chem. Soc. Rev.* **2007**, *36*, 93–104.
[9] S. J. Dalgarno, N. P. Power, J. L. Atwood, *Coord. Chem. Rev.* **2008**, *252*, 825–841.
[10] T. Haino, M. Kobayashi, Y. Fukazawa, *Chem. Eur. J.* **2006**, *12*, 3310–3319.
[11] P. Jin, S. J. Dalgarno, J. L. Atwood, *Coord. Chem. Rev.* **2010**, *254*, 1760–1768.
[12] K. Kobayashi, K. Ishii, S. Sakamoto, T. Shirasaka, K. Yamaguchi, *J. Am. Chem. Soc.* **2003**, *125*, 10615–10624.
[13] G. V. Oshovsky, D. N. Reinhoudt, W. Verboom, *J. Am. Chem. Soc.* **2006**, *128*, 5270–5278.
[14] O. Dumele, N. Trapp, F. Diederich, *Angew. Chem. Int. Ed.* **2015**, *54*, 12339–12344; *Angew. Chem.* **2015**, *127*, 12516–12521.
[15] G. R. Desiraju, P. S. Ho, L. Kloo, A. C. Legon, R. Marquardt, P. Metrangolo, P. Politzer, G. Resnati, K. Rissanen, *Pure Appl. Chem.* **2013**, *85*, 1711–1713.
[16] G. Cavallo, P. Metrangolo, R. Milani, T. Pilati, A. Priimägi, G. Resnati, G. Terraneo, *Chem. Rev.* **2016**, *116*, 2478–2601.
[17] M. Bedin, A. Karim, M. Reitti, A.-C. C. Carlsson, F. Topić, M. Cetina, F. Pan, V. Havel, F. Al-Ameri, V. Sindelar, K. Rissanen, J. Gräfenstein, M. Erdélyi, *Chem. Sci.* **2015**, *6*, 3746–3756.
[18] A. C. C. Carlsson, A. X. Veiga, M. Erdélyi, *Top. Curr. Chem.* **2015**, *359*, 49–76.
[19] A. C. C. Carlsson, J. Gräfenstein, A. Budnjo, J. L. Laurila, J. Bergquist, A. Karim, R. Kleinmaier, U. Brath, M. Erdélyi, *J. Am. Chem. Soc.* **2012**, *134*, 5706–5715.
[20] A.-C. C. Carlsson, K. Mehmeti, M. Uhrbom, A. Karim, M. Bedin, R. Puttreddy, R. Kleinmaier, A. A. Neverov, B. Nekoueishahraki, J. Gräfenstein, K. Rissanen, M. Erdelyi, *J. Am. Chem. Soc.* **2016**, DOI: 10.1021/jacs.6b03842.
[21] L. Koskinen, P. Hirva, E. Kalenius, S. Jääskeläinen, K. Rissanen, M. Haukka, *CrystEngComm* **2015**, *17*, 1231–1236.
[22] C. B. Aakeröy, A. Rajbanshi, P. Metrangolo, G. Resnati, M. F. Parisi, J. Desper, T. Pilati, *CrystEngComm* **2012**, *14*, 6366–6368.
[23] N. K. Beyeh, F. Pan, K. Rissanen, *Angew. Chem. Int. Ed.* **2015**, *54*, 7303–7307; *Angew. Chem.* **2015**, *127*, 7411–7415.
[24] C. B. Aakeröy, P. D. Chopade, C. F. Quinn, J. Desper, *CrystEngComm* **2014**, *16*, 3796–3801.
[25] M. L. Connolly, *J. Mol. Graphics* **1993**, *11*, 139–141.
[26] L. J. Barbour, *J. Supramol. Chem.* **2001**, *1*, 189–191.
[27] J. L. Atwood, L. J. Barbour, *Cryst. Growth Des.* **2003**, *3*, 3–8.
[28] Spartan'14, Wavefunction, Inc., Irvine, USA.

Received: August 10, 2016
Published online: October 6, 2016

© 2016 Wiley-VCH Verlag GmbH & Co. KGaA, Weinheim